

Ammonium perchlorate-based molecular perovskite energetic materials: preparation, characterization, and thermal catalysis performance with MoS₂

Xiaoxia Li, Shuangqi Hu, Xiong Cao, Lishuang Hu, Peng Deng & Zhaobian Xie

To cite this article: Xiaoxia Li, Shuangqi Hu, Xiong Cao, Lishuang Hu, Peng Deng & Zhaobian Xie (2019): Ammonium perchlorate-based molecular perovskite energetic materials: preparation, characterization, and thermal catalysis performance with MoS₂, Journal of Energetic Materials, DOI: [10.1080/07370652.2019.1679281](https://doi.org/10.1080/07370652.2019.1679281)

To link to this article: <https://doi.org/10.1080/07370652.2019.1679281>



Published online: 21 Oct 2019.



Submit your article to this journal [↗](#)



Article views: 27



View related articles [↗](#)



View Crossmark data [↗](#)



Ammonium perchlorate-based molecular perovskite energetic materials: preparation, characterization, and thermal catalysis performance with MoS₂

Xiaoxia Li^a, Shuangqi Hu^a, Xiong Cao^a, Lishuang Hu^a, Peng Deng^b, and Zhaobian Xie^a

^aSchool of Environment and Safety Engineering, North University of China, Taiyuan, China; ^bState Key Laboratory of Explosion Science and Technology, Beijing Institute of Technology, Beijing, China

ABSTRACT

In this study, ammonium perchlorate (AP)-based molecular perovskite structural high-energetic materials (H₂dabco)[NH₄(ClO₄)₃] (DAP) were fabricated and their catalytic performance upon the addition of MoS₂ nanosheets was investigated. The DAP samples were successfully prepared via a self-assembly reaction and their morphology and structure were characterized via scanning electron microscopy, X-ray diffractometry, and Fourier transform infrared spectroscopy. The thermal decomposition performance of a pure DAP sample and of a mixture of DAP with MoS₂ nanosheets were analyzed via differential scanning calorimetry. The results show that DAP has a high thermal stability at its initial decomposition temperature of 319.8°C, and that its apparent decomposition heat measures 4199 J/g. This value is higher than for AP (829.7 J/g). Furthermore, the thermal decomposition peak temperature of DAP upon the addition of 1 wt% and 3 wt% MoS₂ nanosheets decreases from 394.4°C to 343.3°C and 328.8°C, respectively. The investigation of the catalysis thermal performance of DAP may foster its practical application in composite propellant.

KEYWORDS

AP; molecular perovskite; MoS₂ nanosheets; catalysis; thermal decomposition

1. Introduction

The investigation of novel energetic materials with a high-energy and a high-burning rate has a significant impact on the development of composite propellants, which can be used in ballistic missiles, tactical missiles, and launch vehicles. (Cao et al. 2018, 2019; Chen et al. 2017, 2018a; Deng et al. 2017, 2019a, 2019b, 2018; Li et al. 2019) Currently, ammonium perchlorate (AP) is the main component (> 70%) of the composite propellants. (Li, He, and Peng 2015) In recent years, the improvement of the thermal decomposition performance of AP has been the focus of several investigations. The lower initial decomposition temperature of AP was measured in a series of thermal catalysis decomposition studies where different catalysts such as metals, metal oxides, and their derivatives were used. (Chaturvedi and Dave 2013; Chen et al. 2018c; Cui and Wang 2016; Yan et al. 2015) Moreover, nanosized catalysts increase the number of active sites due to their size and surface effects, and this has a significant effect on the thermal decomposition of AP. (Liu et al. 2004; Dey et al. 2015)

However, when compared to the addition of a catalyst, the modification of AP substantially improves the material performance and reduces the content of ineffective components. Chen and coauthors developed a new type of high-energy molecular perovskite material, (H₂dabco)[NH₄(ClO₄)₃] (DAP), which shows a higher exothermic effect than ammonium perchlorate. (Chen

CONTACT Shuangqi Hu ✉ hsq@nuc.edu.cn; Xiong Cao ✉ cx92rl@163.com School of Environment and Safety Engineering, North University of China, Taiyuan, 030051, China

Color versions of one or more of the figures in the article can be found online at www.tandfonline.com/uegm.

This article has been republished with minor change. This change do not impact the academic content of the article.

et al. 2018b) Moreover, the thermal decomposition of the additional ammonium ions produces a higher amount of gas, which is beneficial to increase the flight speed of missiles and launch vehicles. This material can be used as an alternative to ammonium perchlorate to improve propulsion. DAP molecular perovskite is a highly symmetrical eight-sided cubic ternary compound. Its high thermal stability is generated by the Coulomb interaction between the anions and cations in the molecule. By properly reducing the thermal decomposition temperature of DAP the ignition delay time of the propellant can be reduced.

MoS₂ is a type of transition metal sulfide, which is characterized by a layered structure. The upper and lower Mo atomic layers and the middle S atomic layer are held together by a weak van der Waals force and can be stripped into nanosheets. (Zhu et al. 2017) Due to their unique morphological structure and the tunable thickness of its nanosheets, several investigations of the MoS₂ structure have been carried out in the many different fields. (Ejigu et al. 2017; Mo et al. 2019; Parzinger et al. 2017; Que and He 2016; Srikanta, Subrata, and Pathik 2018) However, no previous report elucidating the thermal catalysis of MoS₂ to energetic materials is present in literature. In this study, MoS₂ nanosheets with a large surface area and a high number of edge sites were prepared via a self-assembly reaction to study the thermal catalysis of energetic material.

The results show that the MoS₂ nanosheets may become a new type of catalyst, which effectively improves the thermal performance of DAPs. The thermal decomposition of DAP was carried out by adding 1 wt% and 3 wt% MoS₂ nanosheets, respectively, and the results show that the thermal decomposition temperature of the sample decreases.

2. Experimental

Ammonium perchlorate (AP) was purchased from Nanjing Chemical Reagent Co., Ltd. and perchloric acid (HClO₄) was purchased from Shanghai Wokai Biotechnology Co., Ltd. MoS₂, triethylenediamine (DABCO) and N-methyl pyrrolidone (NMP) were purchased from Shanghai Aladdin Biochemical Technology Co., Ltd.

2.1. Preparation of DAP

DAP were obtained by a self-assembly reaction in an aqueous solution. 1 mmol triethylenediamine and 1 mmol AP were sequentially added to 20 ml deionized water. Then 2 mmol 70 wt% perchloric acid was injected. The mixture was adequately mixed stirred for half an hour at a low rotation speed of 500 rpm at 35°C. After standing at room temperature for several days, DAP samples were obtained by filtration and drying.

2.2. Preparation of MoS₂ Nanosheets

The MoS₂ nanosheets sample was fabricated by liquid ultrasonic exfoliation. 20 mg MoS₂ was added to 20 ml of NMP solution and sonicated by a centrifuge for several days. The unpeeled MoS₂ was removed by low-speed centrifugation at 2000 rpm, and then centrifuged at a high speed of 10,000 rpm to obtain a MoS₂ nanosheets solution. The NMP solvent was removed by washing several times with ethanol, and dried at 60°C to obtain MoS₂ nanosheets sample.

2.3. Sample Characterization

Scanning electron microscopy (SEM) images of all samples were obtained on a Zeiss Sigma microscope. The crystal structure data of DAP, AP and DABCO samples were tested by a DX-2700 X-ray diffractometer (XRD) with Cu-K α radiation (40 kV, 30 mA). Fourier transform infrared (FT-IR) spectrometer of DAP, AP and DABCO samples were recorded in the wavenumbers range from 4000 to 500 cm⁻¹ with

a Nicolet IS50. X-ray photoelectron spectrometer (XPS) were obtained by an ESCALAB 250 photoelectron spectrometer. Raman spectra was collected using a Raman spectrophotometer.

2.4. Catalytic Activity Measurements

Catalytic thermal performance test of MoS_2 for DAP was obtained by Netzsch STA449F3. The MoS_2 nanosheets were uniformly mixed with DAP at a ratio of 1 and 3 wt%, respectively. The treated sample was dried and subjected by differential scanning calorimetry (DSC) at different heating rates of 5, 10, 15, $20^\circ\text{C}\cdot\text{min}^{-1}$ at a temperature range of $40\text{--}500^\circ\text{C}$ in an argon atmosphere of $80\text{ ml}\cdot\text{min}^{-1}$.

3. Results and Discussion

3.1. Characterization of the DAP Sample

The DAP SEM image Figure 1(a) shows that the sample presents a cubic morphology with dimensions in the $300\text{--}500\ \mu\text{m}$ range. The XRD patterns of the DAP, AP, and DABCO samples are shown in Figure 1(b). The position of the diffraction peaks in DAP are different from AP and DABCO, implying the formation of new crystal. The diffraction peaks are located at 21.15° , 24.50° , 27.50° , 36.65° , and 37.15° and they correspond to the (222), (400), (420), (531), and (600) planes, respectively (CCDC No. 1528108). (Chen et al. 2018b)

As Figure 1(c) shows, the FTIR spectrum of AP presents four strong absorption peaks: the features located at 3276 and 1410 cm^{-1} can be attributed to the stretching and the bending vibrations of the ammonium ions, whereas the peak at 620 and 1037 cm^{-1} are attributed to the stretching vibration of the ammonium perchlorate anion. The FTIR spectrum of DABCO presents the stretching and the anti-symmetric stretching vibrations of CH_2 at 2864 and 2932 cm^{-1} . The swing vibration and the scissor vibration of C-H are observed at 1317 and 1460 cm^{-1} , respectively. (Liu et al. 2016) The peaks located at 1055 and 770 cm^{-1} are assigned to the stretching vibrations of C-N and C-C, respectively. A similar pattern is present in the FTIR spectrum of DAP. However, a significant red shift can be observed due to the formation of ligands, which stabilize the structure.

3.2. Characterization of the MoS_2 Nanosheets

The SEM image of the MoS_2 nanosheets is shown in Figure 2(a). The MoS_2 sample was stripped into thin nanosheets with 10 nm thickness, 200 nm width, and 500 nm length. X-ray photoelectron spectroscopy measurements were carried out to characterize their structure. Figure 2(b) shows the $3d_{3/2}$ and $3d_{5/2}$ characteristic peaks, which are located at 229.2 eV and 232.4 eV , respectively, indicating the existence of Mo_4^+ . Figure 2(c) shows the Raman spectrum of the nanosheets: the two features

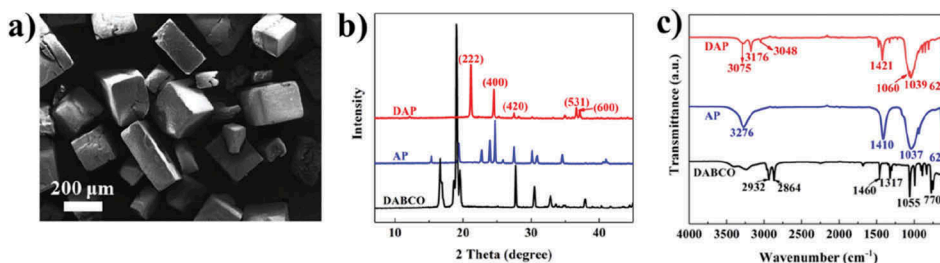


Figure 1. DAP SEM image (a) and XRD pattern (b), FTIR spectrum (c) of DAP, AP and DABCO samples.

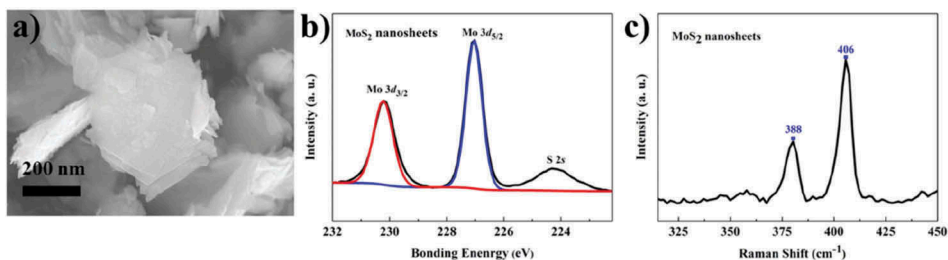


Figure 2. SEM image (a), XPS spectra (b), and Raman spectra (c) of the MoS₂ nanosheets.

located at 388 cm⁻¹ and 406 cm⁻¹ can be assigned to the characteristic peaks of the 2H phase of MoS₂. These observations further demonstrate the successful preparation of the MoS₂ nanosheets.

3.3. Thermal Catalytic Performance of MoS₂ Nanosheets in DAP

The DSC curves show the thermal decomposition of AP and DAP **Figure 3(a)** measured with a heating rate of 10°C·min⁻¹. The thermal decomposition curve of AP presents two exothermic peaks, which are located at 307.9°C and 441.5 °C. However, DAP presented only an exothermic process with an exothermic peak, demonstrating that AP and DAP were two different substances. The result shows that the initial thermal decomposition temperature of DAP (319.8°C) is much higher than the initial thermal decomposition temperature of AP (273.98°C). The apparent decomposition heat of AP with two exothermic peaks was 829.7 J/g, while the apparent decomposition heat of DAP is 4199 J/g, which indicates that DAP is more advantageous in terms of energy.

The combustion process of the composite propellant was affected by the thermal decomposition characteristics of ammonium perchlorate. To improve the combustion of the composite propellant, different catalysts were often added to the AP. As shown in **Table 1**, the catalyst can decrease the exothermic peak temperature of AP, while giving a higher apparent decomposition heat. However, it was still lower compared to the thermal decomposition of DAP without and with MoS₂ nanosheets.

In order to study the effect of a catalyst on the thermal decomposition of DAP, 1 wt% and 3 wt% MoS₂ nanosheets were added to the DAP sample. The thermal decomposition curves of pure DAP and a mixture of DAP and MoS₂ nanosheets are shown in **Figure 3(b)**. The thermal decomposition

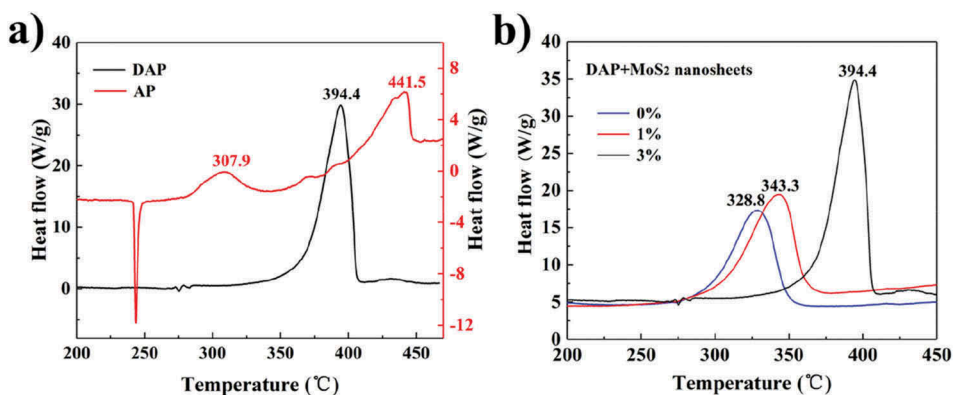


Figure 3. (a) DSC curves of the thermal decomposition of AP and DAP, and (b) DSC curves of a pure DAP sample and a mixture of DAP with 1 wt% and 3 wt% MoS₂ nanosheets, respectively, recorded at a heating rate of 10°C·min⁻¹.

Table 1. Comparison of catalytic activity of different catalysts reported on the thermal decomposition of AP and peak temperature T_p and apparent decomposition heat ΔH of DAP sample.

Sample	T_p (°C)	ΔH (J·g ⁻¹)	Reference
g-C ₃ N ₄ (10%)	384.4	1362.6	Li et al. 2015
Ni powder (4%)	364.3	1320	Liu et al. 2004
(3,5-DNB) ₂ Co (4%)	318.5	942	Zhao et al. 2016
rGO/CuFe ₂ O ₄ (3%)	329.1	1523.5	Wang and Zhang, 2018
g-C ₃ N ₄ /rGO/MnO ₂ (2%)	364.8	1669.2	Xu et al. 2017
Fe ₂ O ₃ /rGO/MnO ₂ (1%)	380.8	1897.5	Dey et al. 2015
DAP	394.4	4199	This work
DAP+3%	328.8	2692	This work

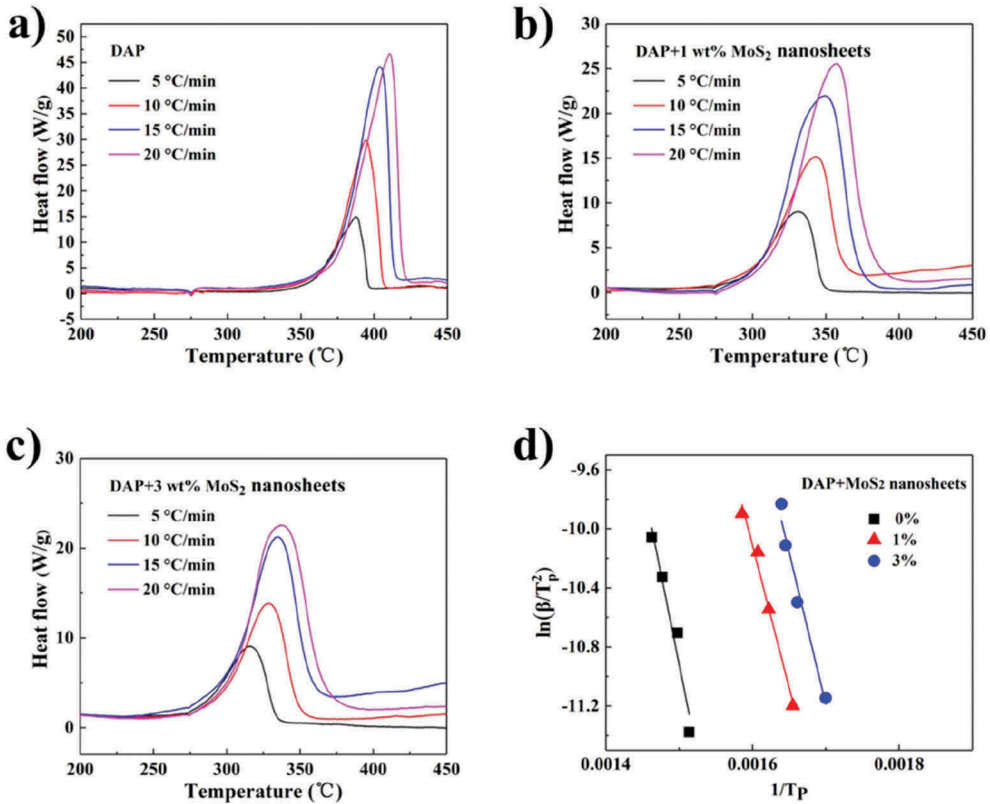


Figure 4. DSC curves of pure DAP (a) and a mixture of DAP with 1 wt% (b) and 3 wt% (c) MoS₂ nanosheets at different heating rates (5, 10, 15 and 20°C·min⁻¹). Dependence of $\ln(\beta/T_p^2)$ on $1/T_p$ (d) for DAP and a mixture of DAP with 1 wt% and 3 wt% MoS₂ nanosheets. Lines in the Figure 5d display the linear fitting result of the tested data.

peak temperature of DAP decreases to 343.3°C and 328.8°C upon the addition of 1wt% and 3 wt% MoS₂ nanosheets, respectively. This shows that as the quantity of MoS₂ nanosheets in the DAP sample increases, the exothermic its peak temperature decreases.

The DSC curves Figure 4(a-c) of thermal decomposition of pure DAP and a mixture of DAP and MoS₂ nanosheets at different heating rates of 5, 10, 15, 20°C·min⁻¹ were obtained. The apparent activation energy E_a , an important parameter of the thermal decomposition reaction, was obtained according to the peak temperature value of the thermal decomposition (Table 2) and Kissinger equation (1).

Table 2. The exothermic peak temperature (T_p) and the activation energy (E_a) of DAP and DAP/MoS₂ nanosheets.

Sample	T_p (°C)				E_a (kJ·mol ⁻¹)
	5°C·min ⁻¹	10°C·min ⁻¹	15°C·min ⁻¹	20°C·min ⁻¹	
DAP	387.5	394.4	403.9	410.6	205.4
DAP/1% MoS ₂	331.1	343.3	349.0	357.5	160.4
DAP/3% MoS ₂	315.1	328.8	334.7	336.8	170.9

$$\ln\left(\frac{\beta}{T_p^2}\right) = -\frac{E_a}{RT_p} + \ln\left(\frac{AR}{E_a}\right) \quad (1)$$

Where T_p is the peak temperature, β is the heating rate, R is the ideal gas constant (8.314 J·mol⁻¹·K⁻¹), A is frequency factor, and E_a is the activation energy.

As shown in Figure 4(d), experiments measured different heating rates β , plotting $\ln(\beta/T_p^2)$ versus $1/T_p$, and the activation energy E_a can be obtained from the slope of the line. As shown in Table 2, the activation energy E_a of DAP (205.4 kJ·mol⁻¹) decreased to 160.4 kJ·mol⁻¹ and 170.9 kJ·mol⁻¹ with the addition of 1 wt% and 3 wt% MoS₂ nanosheets, which revealed that MoS₂ nanosheets is a type of excellent thermal catalyst for the thermal decomposition of DAP

4. Conclusions

In this work the DAP samples were prepared via a self-assembly reaction. A morphological and the structural characterization were carried out and the results show that the samples present a cubic morphology. DAP has a high apparent decomposition heat, which is higher than the value measured for AP (829.7 J/g). The addition of 1 wt% and 3 wt% MoS₂ two-dimensional nanomaterials significantly decreases the thermal decomposition peak temperature of DAP from 394.4°C to 343.3°C and 328.8°C, respectively. These observations show that DAP can be used as a high energetic material in composite propellants in a variety of applications.

Acknowledgments

This work was supported by Natural Science Foundation of China (No: 50972016). And authors thank Prof. Weixiong Zhang and Ph. D. Shaoli Chen (School of Chemistry, Sun Yat-Sen University) for supports and help.

Conflicts of interest

There are no conflicts to declare.

Funding

This work was supported by the National Natural Science Foundation of China [21975227]; Scientific and Technological Innovation Programs of Higher Education Institutions in Shanxi (STIP).

References

- Cao, X., P. Deng, S. Hu, L. Ren, X. Li, P. Xiao, and Y. Liu. 2018. Fabrication and characterization of nanoenergetic hollow spherical hexanitrostibene (HNS) derivatives. *Nanomaterials* 8:336. doi:10.3390/nano8050336.
- Cao, X., Y. P. Shang, K. J. Meng, G. D. Yue, L. Y. Yang, L. Yang, P. Deng, and L. S. Hu. 2019. Fabrication of three-dimensional TKX-50 network-like nanostructures by liquid nitrogen-assisted spray freeze drying method. *Journal of Energetic Materials*. doi: 10.1080/07370652.2019.1585491.

- Chaturvedi, S., and P. N. Dave. 2013. A review on the use of nanometals as catalysts for the thermal decomposition of ammonium perchlorate. *Journal of Saudi Chemical Society* 17:135–49. doi:10.1016/j.jscs.2011.05.009.
- Chen, J., S. He, B. Huang, P. Wu, Z. J. Qiao, J. Wang, L. Y. Zhang, G. C. Yang, and H. Huang. 2017. Enhanced thermal decomposition properties of CL-20 through space-confining in three-dimensional hierarchically ordered porous carbon. *ACS Applied Materials & Interfaces* 9:10684–91. doi:10.1021/acsami.7b00287.
- Chen, S. L., Y. Shang, C. T. He, L. Y. Sun, Z. M. Ye, W. X. Zhang, and X. M. Chen. 2018a. Optimizing the oxygen balance by changing the A-site cations in molecular perovskite high-energetic materials. *CrystEngComm* 20:7458–63. doi:10.1039/C8CE01350K.
- Chen, S.-L., Z.-R. Yang, B.-J. Wang, Y. Shang, L.-Y. Sun, C.-T. He, H.-L. Zhou, W.-X. Zhang, and X.-M. Chen. 2018b. Molecular perovskite high-energetic materials. *Science China Materials* 61:1123–28. doi:10.1007/s40843-017-9219-9.
- Chen, Y., K. Ma, J. Wang, Y. Gao, X. Zhu, and W. Zhang. 2018c. Catalytic activities of two different morphological nano-MnO₂ on the thermal decomposition of ammonium perchlorate. *Materials Research Bulletin* 101:56–60. doi:10.1016/j.materresbull.2018.01.013.
- Cui, P., Wang, A.J. 2016. Synthesis of CNTs/CuO and its catalytic performance on the thermal decomposition of ammonium perchlorate. *J. Saldi. Chem. Soc.* 20, 343-348. doi:10.1016/j.jscs.2014.09.010.
- Deng, P., H. Ren, and Q. J. Jiao. 2019a. Enhanced the combustion performances of ammonium perchlorate-based energetic molecular perovskite using functionalized graphene. *Vacuum*, 169:108882. doi: 10.1016/j.vacuum.2019.108882.
- Deng, P., H. Ren, Q. J. Jiao. 2019b. Enhanced thermal decomposition performance of sodium perchlorate by molecular assembly strategy, IONICS, Accepted.
- Deng, P., J. J. Xu, S. C. Li, S. L. Huang, H. B. Zhang, J. X. Wang, and Y. Liu. 2018. A facile one-pot synthesis of monodisperse hollow hexanitrostilbene-piperazine compound microspheres. *Materials Letters* 214:45–49. doi:10.1016/j.matlet.2017.11.104.
- Deng, P., Y. Liu, P. Luo, J. Wang, Y. Liu, D. Wang, and Y. He. 2017. Two-steps synthesis of sandwich-like graphene oxide/LLM-105 nanoenergetic composites using functionalized graphene. *Materials Letters* 194:156–59. doi:10.1016/j.matlet.2017.02.038.
- Dey, A., J. Athar, P. Varma, H. Prasant, A. K. Sikder, and S. Chattopadhyay. 2015. Graphene-iron oxide nanocomposite (GINC): an efficient catalyst for ammonium perchlorate (AP) decomposition and burn rate enhancer for AP based composite propellant. *RSC Advances* 5:1950–1960.
- Ejigu, A., I. A. Kinloch, E. Prestat, and R. Dryfe. 2017. A simple electrochemical route to metallic phase trilayer MoS₂: evaluation as electrocatalysts and supercapacitors. *Journal of Materials Chemistry A* 5:11316–30. doi:10.1039/C7TA02577G.
- Li, Q., Y. He, and R. F. Peng. 2015. Graphitic carbon nitride (g-C₃N₄) as a metal-free catalyst for thermal decomposition of ammonium perchlorate. *RSC Advances* 5:24507–12. doi:10.1039/C5RA01157D.
- Li, X. D., B. Huang, R. Li, H. P. Zhang, W. Z. Qin, Z. Q. Qiao, Y. S. Liu, and G. C. Yang. 2019. Laser-ignited relay-domino-like reactions in graphene oxide/CL-20 films for high-temperature pulse preparation of Bi-layered photothermal membranes. *Small* 15:1900338–47. doi:10.1002/smll.v15.20.
- Liu, E., B. Sarkar, Z. Chen, and R. Naidu. 2016. Decontamination of chlorine gas by organic amine modified copper-exchanged zeolite. *Microporous and Mesoporous Materials* 225:450–55. doi:10.1016/j.micromeso.2016.01.023.
- Liu, L. L., F. S. Li, L. H. Tan, M. Li, and Y. Yang. 2004. Effects of nanometer Ni, Cu, Al and NiCu powders on the thermal decomposition of ammonium perchlorate. *Propellants, Explosives, Pyrotechnics* 29:34–38. doi:10.1002/(ISSN)1521-4087.
- Mo, Z, H. Xu, Z. Chen, X. She, Y. Song, J. Lian, X. Zhu, P. Yan, Y. Lei, S. Yuan, and H. Li. 2019. Construction of MnO₂/monolayer g-c 3 n 4 with Mn vacancies for Z-scheme overall water splitting. *Applied Catalysis B: Environmental* 241, 452–460. doi: 10.1016/j.apcatb.2018.08.073.
- Parzinger, E., E. Mitterreiter, M. Stelzer, F. Kreupl, and U. Wurstbaue. 2017. Hydrogen evolution activity of individual mono-, bi-, and few-layer MoS₂ towards photocatalysis. *Applied Materials Today* 8:132–40. doi:10.1016/j.apmt.2017.04.007.
- Que, W. X., and Z. L. He. 2016. Molybdenum disulfide nanomaterials: Structures, properties, synthesis and recent progress on hydrogen evolution reaction. *Applied Materials Today* 3:23–56. doi:10.1016/j.apmt.2016.02.001.
- Srikanta, K., B. Subrata, and K. Pathik. 2018. A comparison of temperature dependent photoluminescence and photo-catalytic properties of different MoS₂ nanostructures. *Applied Surface Science* 455:379–91. doi:10.1016/j.apsusc.2018.05.204.
- Wang, W. R., and D. X. Zhang. 2018. Facile preparation of rGO/MFe₂O₄ (M = Cu, Co, Ni) nanohybrids and its catalytic performance during the thermal decomposition of ammonium perchlorate. *RSC Advances* 8 :32221–30. doi:10.1039/C8RA04412K.
- Xu, J. H., D. N. Li, Y. Chen, L. H. Tan, B. Kou, F. S. Wang, W. Jiang, and F. S. Li. 2017. Constructing sheet-on-sheet structured graphitic carbon nitride/reduced graphene oxide/layered MnO₂ ternary nanocomposite with outstanding catalytic properties on thermal decomposition of ammonium perchlorate. *Nanomaterials* 7:450–63. doi:10.3390/nano7120450.

- Yan, D., H. Y. Zhao, Y. Liu, X. Wu, and J. Y. Pei. 2015. Shape-controlled synthesis of cobalt particles by a surfactant-free solvothermal method and their catalytic application to the thermal decomposition of ammonium perchlorate. *CrystEngComm* 17:9062–69. doi:10.1039/C5CE01424G.
- Zhao, W. Y., T. L. Zhang, N. M. Song, L. N. Zhang, Z. K. Chen, Y. Li, and Z. N. Zhou. 2016. Assembly of composites into a core-shell structure using ultrasonic spray drying and catalytic application in the thermal decomposition of ammonium perchlorate. *RSC Advances* 6:71223–31. doi:10.1039/C6RA08150A.
- Zhu, J. Q., Z. C. Wang, H. Yu, N. Li, J. Zhang, J. L. Meng, M. Z. Liao, J. Zhao, X. B. Lu, L. J. Du, R. Yang, D. X. Shi, Y. Jiang, and G. Y. Zhang. 2017. Argon plasma induced phase transition in monolayer MoS₂. *Journal of the American Chemical Society* 139:10216–19. doi:10.1021/jacs.7b05765.